Preliminary characterisation of nanotubes connecting T-cells and their use by HIV-1

Simon Lachambre, Christophe Chopard, Bruno Beaumelle

Preliminary characterization of nanotubes connecting T-cells and of their use by HIV-1

Simon Lachambre, Christophe Chopard and Bruno Beaumelle
CPBS, UMR 5236 CNRS-Université de Montpellier, 1919 Route de Mende, 34293 Montpellier

Email bruno.beaumelle@cpbs.cnrs.fr

Biology of the Cell (2014) 106, 1–11
DOI: 10.1111/boc.201400037

Abstract

Background information. Cells, especially those of the immune system, can form long and thin connections termed tunneling nanotubes (TNTs). These structures can reach >100 μm in length and, in T-cells, contain actin but no tubulin and are not open ended. T-cell TNTs were found to form following cell contact and to enable the transfer of HIV-1 from an infected- to a connected-T-cell. TNTs are poorly characterized at molecular level.

Results. We found Rab11 and tetraspanins, especially CD81, all along T-cells TNTs while Rab4 and Rab35 were absent from these structures. Regarding actin cytoskeleton regulators, Exo70, N-WASP and especially ezrin accumulated at the level of the TNT tip that contacts the connected cell. Phosphoinositides such as $PI(4,5)P_2$ were also concentrated at this level together with HIV-1 Gag. Gag spots on cells and TNTs were essentially immobile, and likely correspond to area of Gag multimerisation for budding to form virus-like particles. Mobility of $PH_{PLC\delta}$, a specific probe for $PI(4,5)P_2$ was reduced > 3-fold at the level of TNT basis or tip compared to the cell body.

Conclusion. Our study identified the TNT tip as an active zone of actin cytoskeleton reorganisation with the presence of ezrin, Exo70, N-WASP and $PI(4,5)P_2$. The latter is also known to enable HIV-1 Gag recruitment for viral budding, and the presence of Gag at this level, contacting the connected cell indicates that the TNT tip is also a favourite place for HIV-1 assembly and budding.

Introduction

Cell contacts within the immune system are not restricted to neighbour cells and, during the recent years, evidence for long distance connections between distant cells accumulated. These thin structures have lengths of up to several cell diameters and were termed tunelling nanotubes (TNTs). They are longer than filopodia that are smaller than cell diameter (Sherer, et al., 2007), and were first described in PC12 cells. In this cell type, TNTs have a diameter of 50-200 nm and contain actin but no microtubules (Rustom, et al., 2004). TNTs were observed between various immune cells, such as B-cells and macrophages; TNTs of up to 140 µm in length were observed in this pioneer study (Onfelt, et al., 2004). As reviewed recently (Abounit and Zurzolo, 2012), TNTs are not all identical. For instance, macrophages can produce two types of TNTs, thin ones (~0.3 µm in diameter) containing F-actin only and thick ones (~ 0.8 µm in diameter) that contain both F-actin and tubulin. The role of these different TNTs appears different since only small ones enabled bacteria to "surf" at their surface before phagocytosis by the destination cell, while only thick ones allowed the transfer of organelles such as mitochondria, late endosomes or lysosomes. TNTs were observed between macrophages whether they were plated on fibronectin or not (Onfelt, et al., 2006). This was not the case for T-cells that require adsorption onto fibronectin-coated substratum to produce TNTs. T-cells TNTs were found to contain actin but no tubulin and do not form open-ended tunnels since no intercellular transfer of cytosolic GFP or calcium flux was observed through these connections. Membrane proteins such as GPI-GFP or type I membrane proteins were not transferred either, indicating the absence of membrane continuity between the connected cells. No specific structure was observed by transmission electron microscopy at the site where the two parts of the TNTs interact (Sowinski, et al., 2008).

There is evidence for the existence of TNTs *in vivo*, between dendritic cells in the cornea for instance (Chinnery, et al., 2008). This type of membrane extensions also plays a crucial role during *Drosophila* development (De Joussineau, et al., 2003). Moreover, TNTs are exploited by several pathogens such as HIV-1. The use of humanized mice and multiphoton intravital microscopy showed that HIV-1 infected T-cells form TNT-like structures *in vivo*, and that HIV-1 uses these cell extensions to disseminate within lymph nodes (Murooka, et al., 2012). Such HIV-1 transfer from an infected T-cell to an uninfected one *via* TNTs was also observed *in vitro*, using conventional cell culture (Sowinski, et al., 2008). Since, as indicated above, T-cells TNTs do not allow the direct transfer of membrane protein from one cell to the other, infection involves a cell-free (although presumably attached) intermediate. Indeed, a fusion inhibitor or neutralizing antibodies against gp120 or CD4 (respectively the viral glycoprotein and its receptor) prevented transmission (Sowinski, et al., 2008). It should also be noted that T-cell infection by HIV-1 did not induce TNT formation and that preventing HIV-1 transfer did not affect TNT number either (Sowinski, et al., 2008), indicating that TNTs are different from filopodia that are induced by HIV-1 Nef (Nobile, et al., 2010), or those stabilized by Env that fall apart in the presence of neutralizing anti-Env antibodies (Sherer, et al., 2007).

Despite their recognized role in HIV-1 transmission between T-cells, TNTs are poorly characterized at the molecular level. For instance it is not known whether cell membrane molecules involved in HIV-1 budding are present in TNTs. The first step in HIV-1 virion formation is the recruitment to the plasma membrane of the major HIV-1 structural protein, Gag. Expression of this single viral protein is sufficient to drive the assembly of virus-like particles (VLPs) that are morphologically similar to HIV-1 immature virions (Fuller, et al., 1997). The most recent data showed that VLP budding involves the same machinery as the one used by the entire virus (Van Engelenburg, et al., 2014). This key step of HIV-1 infection cycle has been recently reviewed (Bell and Lever, 2013). An essential player to insure Gag targeting to the plasma membrane is phosphatidylinositol (4,5) bisphosphate ($PI(4,5)P_2$). This phosphoinositide is specifically associated with the inner leaflet of the plasma membrane where it assembles in microdomains of ~73 nm in size as determined using super-resolution microscopy (van den Bogaart, et al., 2011). Tetraspanins are a family of four transmembrane domain-containing proteins. They interact laterally with each other to form tetraspanin webs, also termed tetraspanin-enriched microdomains (Espenel, et al., 2008) that were also found to colocalize with assembling Gag at the plasma membrane (Ono, 2010). Moreover tetraspanins, especially

CD81, negatively regulate HIV-1 cell to cell transmission but not cell-free virion infectivity (Krementsov, et al., 2009).

Here we found that $PI(4,5)P_2$ and tetraspanins are present within TNTs, but with different localization. $PI(4,5)P_2$ was found with Gag at the level of the TNT tip that establishes contact with the connected cell, while tetraspanins were observed all along the TNTs.

Results

Specificity of TNT imaging using fluorescence microsocopy

Throughout these studies we used Jurkat cells that were plated onto fibronectin coated coverslips before overnight incubation and either live-imaging or fixation with paraformadehyde with or without glutaraldehyde (Sowinski, et al., 2011). We did not find that glutaraldehyde addition improved TNT preservation as long as paraformaldehyde was added at low concentration (0.1%) during cell washes before conventional fixation with 3.7% paraformaldehyde. Live imaging of T-cell TNTs is difficult because these tubes connect essentially spheric cells by their equatorial plane and therefore nanotubes do not lay on the substrate. They thus move, are fragile and sensitive to light exposure (Abounit and Zurzolo, 2012). Indeed, strong illumination such as those needed for FRAP for instance can induce TNT movements.

Although previous reports indicated that 13% of Jurkat cells were connected by TNTs (Sowinski, et al., 2008) we never found more than 1/10 000 of Jurkat cells with TNTs and therefore could not reliably quantify them. Hence, although we found several cell molecules concentrated within TNTs, this lack of quantitative assay prevented us from studying their role in TNT formation, by using siRNAs for instance. Throughout this study we avoid imaging as TNT membranous tethers that connect daughter cells at the end of cell division, before abscission. These connections can be identified by the presence of a characteristic midbody that causes a bulge in the middle of the tube (Sowinski, et al., 2008). Finally, please note that because TNTs are thin structures that contain a limited amount of fluorophores, their visualization usually requires acquisition settings such as the signal from the cell body is saturated.

Absence of lipophilic dye transfer through nanotubes

Jurkat T-cells were labelled with a lipophilic dye (DiI or DiD (Sowinski, et al., 2011)) before mixing the two populations, plating onto fibronectin-coated coverslips, overnight incubation, fixation and observation by confocal microscopy. As observed before (Sowinski, et al., 2011), T-cells can form two types of TNTs. We found that most of them are extensions from a single cell only while others are made of extensions from the two connected cells. Lipophilic tracers were not transferred from one cell to the other *via* TNTs indicating that membrane discontinuity is preserved at the junction between connected cells (Fig.1A).

Actin, ezrin and N-WASP are present in TNTs

As reported earlier (Sowinski, et al., 2011), T-cell TNTs contain actin (Fig.1F) but few α tubulin (Fig.1B), indicating that these structures are devoid of microtubules. We then examined whether regulators of actin polymerisation were present within TNTs. Cdc42 and Rac GTPases are key regulators of membrane extension such as lamellipodia and filopodia (Heasman and Ridley, 2008), and we found them at the basis of TNTs only, close to the cell body of the transfected cell (Fig.1E and F). N-WASP is involved in connections between the membrane and the cytoskeleton and has been shown to localize to certain types of filopodia (Takenawa and Suetsugu, 2007). We found it within TNTs (Fig.1D), not only at the basis but also at the tip of the TNT, indicating that active actin polymerization takes place at these levels. We also studied the localization within TNTs of ezrin, a member of the ezrin-radixin-moesin (ERM) family. ERM proteins are involved in membrane-cytoskeleton interaction and in the organization of membrane domains (Fehon, et al., 2010). T-cells express no radixin, traces of ezrin and a lot of moesin (Faure, et al., 2004). We found that ezrin-GFP, a chimera validated earlier (Lamb, et al., 1997), accumulated at the basis and, interestingly, at the tip of the TNT (Fig.1C).

$PI(4,5)P_2$ and $PI(3,4,5)P_3$ are enriched at the tip of the TNT

Because ezrin is activated by phosphorylation and binding to $PI(4,5)P_2$ (Fehon, et al., 2010) we examined, using a GFP chimera of the PH domain of PLCδ that specifically binds this phosphoinositide (Varnai and Balla, 1998), whether it was present within TNTs. We found that $PI(4,5)P_2$ is specifically enriched in the distal part of the TNT at the site of junction with the contacted cell (Fig.2), *i.e.* where ezrin accumulated (Fig.1C). The other phosphoinositide $PI(3,4,5)P_3$, localized with the Akt PH domain (Astoul, et al., 2001), was also present at the TNT tip (Fig.2). The specific enrichment of these probes at the TNT tip was observed in 65-70% of the TNTs we observed. It should be noted that this value is likely an underestimate because some TNT tips were either not in the confocal section or difficult to identify due to signal saturation at the target cell periphery.

Cytoplasmic proteins have access to TNT

As observed before (Sowinski, et al., 2011), cytoplasmic proteins such as GFP or a GFP chimera of the R40L mutant of $PH_{PLC\delta}$ that is unable to bind $PI(4,5)P_2$ (Varnai and Balla, 1998) were found within TNTs (Fig.3). The fact that the $PH_{PLC\delta}$ mutant was present throughout the TNT length (Fig.3) shows that the specific accumulation of WT $PH_{PLC\delta}$ at the TNT tip (Fig.2) is due to its capacity to bind $PI(4,5)P_2$.

Are membrane-deforming proteins present within TNTs?

We then studied the localization in TNTs of proteins known to deform membrane and induce filopodia. Missing-in-metastasis (MIM) is a member of the BAR (Bin, Amphiphysin, Rvs) domain superfamily of proteins. MIM is an actin-binding protein that directly binds $PI(4,5)P_2$ and deforms membrane by inducing membrane protrusions. This activity is due to the presence of an I-BAR domain at its N-terminus (Zhao, et al., 2011). As observed in other cell types (Zhao, et al., 2011), expression of a GFP chimera of MIM I-BAR domain induced dramatic changes in T-cell shape, with the generation of several filopodia (Fig.4). Most often, these elongations did not contact other cells and are therefore different from *bona fide* TNTs. This result suggests that MIM is not responsible for TNT generation, although it does not rule out that MIM could be present in TNTs. Exo70 is another protein able to induce filopodia upon overexpression within cells (Zhao, et al., 2013). Its transient expression in T-cells did not lead to the formation of filopodia although exo70 was observed within TNTs (Fig.4). T-cells are largely devoid of M-Sec (Ohno, et al., 2010), nevertheless transient expression of M-Sec in macrophages induces the formation of numerous membrane protrusions that connect cells, contain actin but not microtubules and allow calcium flux (Hase, et al., 2009). We found that transfected GFP-M-Sec did not localize to TNTs and did not induce cell protrusions in T-cells (Fig.4). This result is consistent with previous observations indicating that TNTs are different structures in macrophages (Hase, et al., 2009) and T-cells (Sowinski, et al., 2011). Hence, of the three proteins able to induce membrane curvature that we tested, only Exo70 seems to localize to *bona fide* TNTs. This result is consistent with the capacity of $PI(4,5)P_2$ to recruit Exo70 to the plasma membrane (Liu, et al., 2007). Moreover, Exo70 is known to stimulate the Arp2/3 complex to promote actin filament nucleation and branching (Liu, et al., 2012). Its localization to the TNT tip confirms that active actin polymerisation likely takes place at this level.

T-cells TNTs are essentially devoid of elements of the exocytic and endocytic pathway

It is still unclear whether T-cells TNTs contain elements of the exocytic or endocytic pathway. To examine this point we first transiently expressed YFP-KDEL (Bannai, et al., 2004). We did not find significant amount of this ER tracer within TNTs (Fig.5). Regarding the endocytosis pathway we used different Rab proteins as markers (Mitra, et al., 2011). In Jurkat cells, Rab4 is concentrated within the perinuclear recycling compartment. Rab11 is observed within these recycling endosomes, but also to some extend at the plasma membrane. Rab5 is associated with endosomal compartments dispersed throughout the cytoplasm, while Rab35 essentially localized to the plasma membrane (SupFig.1). We observed Rab4 and Rab35 at a low level within TNTs (Fig.5). Similar data were obtained for Rab5 (data not shown). Rab11 was more

concentrated in TNTs but showed a linear labelling pattern consistent with plasma membrane labelling and not accumulation within intra-TNT structures. Although it was somehow surprising to find that Rab11 is more concentrated than Rab35 within TNTs, these data suggest that endocytic traffic does not take place within TNTs. They were confirmed when fluorescent transferrin was used (see below). This interpretation is also consistent with electron microscopic examination of these cell extensions that did not show evidence for vesicular or cisternal structures within T-cell TNTs (Sowinski, et al., 2011).

T-cells TNTs are enriched in tetraspanins

Tetraspanins were good candidates to associate with TNT because the tetraspanin web is known to interact with ERM proteins (Charrin, et al., 2009; Sala-Valdes, et al., 2006) that we found in TNTs (Fig.1C). Indeed we found that both CD9 and CD81 accumulated within TNTs. More specifically, CD81-mCherry was even more sensitive than phalloidin conjugates to insure sensitive visualization of these structures (Fig.6). Although CD81 could be observed with $PH_{PLC\delta}$ at the level of the TNT tip, tetraspanins did not show the specific accumulation at the TNT apex that was observed for ezrin (Fig.1C) or $PI(4,5)P_2$ (Fig.2).

HIV-1 Gag accumulates at the TNT tip

TNTs were previously found to allow HIV transfer to the connected cell but the mechanistic of HIV-1 targeting to these structures was not studied (Sowinski, et al., 2011). To examine this point we used a Gag-GFP chimera that can form VLPs just as native Gag (Hermida-Matsumoto and Resh, 2000). At low expression level, Gag-GFP showed a diffuse cytosolic labelling with a few spots on the plasmalemma (Fig.7A), while at higher expression level these spots became more numerous (Fig.7B). When T-cells were cotransfected with CD81-mCherry and Gag-GFP we found that Gag localized to TNTs, as observed before with the complete virus (Sowinski, et al., 2011). More specifically, we most often found Gag accumulation at the TNT tip, at the site of contact with the connected cell(s) (Fig.7B), just where $PI(4,5)P_2$ is present (Fig.2). This observation is consistent with the crucial role of this phosphoinositide for Gag targeting to the plasma membrane and for HIV-1 budding (Bell and Lever, 2013). Along the same lines, the partial colocalization of Gag with CD81 at the TNT tip (Fig.7B, inset) is consistent with the CD81 colocalization with $PH_{PLC\delta}$ at this level (Fig.6).

Mobility of $PI(4,5)P_2$ and HIV-1 Gag on TNTs

Does HIV-1 move along TNTs, by viral "surfing" for instance (Lehmann, et al., 2005) or is it assembled at different sites along these structures, especially at the tip? To examine this point we used fluorescence recovery after photobleaching (FRAP). As observed before in HeLa cells (Helma, et al., 2012; Jouvenet, et al., 2008), in most cases (>80%), we did not observe significant fluorescence recovery following bleaching of Gag-GFP spots at the plasma membrane (not shown) or TNTs of Jurkat cells (Fig.8A). This result indicates that these spots are stable and probably correspond to VLP assembly sites. To assess whether this immobility was due to a restricted diffusion of $PI(4,5)P_2$, we monitored its mobility using $PH_{PLC\delta}$-GFP. This probe was found to diffuse rapidly with an apparent diffusion coefficient (D) ~ 1.2 $\mu m^2/s$ at the plasma membrane of HEK cells (Hammond, et al., 2009). This value is similar to those obtained for a fluorescent analog of $PI(4,5)P_2$ (Golebiewska, et al., 2008; Golebiewska, et al., 2011). We accordingly observed D~1.1 $\mu m^2/s$ at the surface of Jurkat cells, and similar values were obtained in the middle of TNTs, indicating that membrane curvature did not significantly affect D measurements in this experimental system (Fig.8B). Nevertheless, D was significantly decreased to D~0.3 $\mu m^2/s$ at the level of cell extensions or at the tip or basis of TNTs. Hence, although $PI(4,5)P_2$ mobility was reduced at the level of TNT ends it remained significant and is not responsible for the immobility of Gag spots on these structures.

Discussion

Evidence is accumulating that TNTs play a major role in cell communication within elaborated organs (Davis and Sowinski, 2008). In the case of T-cells, TNT-like structures have been shown to promote HIV-1 dissemination within lymph nodes *in vivo* (Murooka, et al., 2012). This mode of viral transmission seems to be especially relevant for T-tropic viruses such as HIV-1 and HTLV-1 whose dissemination in the body

essentially takes place *via* cell contacts (Igakura, et al., 2003; Martin-Serrano and Neil, 2011). Although TNTs were known to contain cytosolic proteins, actin but not tubulin (Sowinski, et al., 2011), little was known regarding the other structural elements that make up T-cell TNTs. Among the different markers we used for the endocytic or the exocytic pathway, none of them was significantly concentrated within TNTs, indicating that these cell extensions do not contain intermediates of the endocytic or exocytic pathways. We nevertheless found that Rab11 and tetraspanins, especially CD81, were present all along the TNT membrane. This localization was clearly different from that of $PI(4,5)P_2$, ezrin and HIV-1 Gag that were enriched at the TNT apex, where contact with the connected cell takes place. The TNT tip thus seems to be a specific domain of this structure.

The significant reduction in $PI(4,5)_2$ mobility within TNTs ends (*i.e.* basis and tip) could indicate the presence of a fence limiting $PI(4,5)_2$diffusion as is the case at the level of the phagocytic cup (Golebiewska, et al., 2011) or, more probably, that this phosphoinositide interacts with proteins at this level. Indeed, we found several $PI(4,5)P_2$ binding proteins involved in actin cytoskeleton organization such as ezrin (Fehon, et al., 2010), N-WASP (Thrasher and Burns, 2010) and exo70 (Liu, et al., 2007) at the TNT tip. It is well established that areas of the plasma membrane enriched in $PI(4,5)P_2$ correspond to places where active actin-cytoskeleton remodeling takes place (Di Paolo and De Camilli, 2006).

The localisation of ezrin within TNTs agrees well with the data from a pioneer study that localized moesin, another ERM protein, to dynamic filopodia (Amieva and Furthmayr, 1995). Moreover, $PI(4,5)P_2$ enables Gag targeting to the plasma membrane for HIV-1 budding (Bell and Lever, 2013; Martin-Serrano and Neil, 2011; Ono, 2010). ERM proteins are incorporated within HIV-1 virions during budding, with ezrin and moesin present at a level of ~2 molecules /100 Gag (Ott, et al., 1996). It was therefore not surprising to find $PI(4,5)P_2$, ezrin and Gag in the same place in TNTs. This observation strongly suggests that the TNT tip is a productive site for HIV-1 assembly to infect the connected cell, a kind of "mini" virological synapse. The fact that VLP assembly sites are immobile on TNTs suggests that Gag monomers diffuse through the TNT lumen, just as it is the case for cytosolic proteins, before being recruited by $PI(4,5)P_2$ at the TNT tip for budding in proximity of the connected cell. Nevertheless, our data obtained using VLPs do not exclude that HIV-1 could also be transported on the TNT surface *via* the envelope protein gp120.

The partial colocalization of the tetraspanin CD81 with Gag we observed at the TNT tip (Fig.7B, inset) is consistent with the reported interaction of CD81 with PI-4 kinase, a key enzyme in $PI(4,5)P_2$ synthesis (Berditchevski, et al., 1997). Moreover, the tetraspanin web interacts with ERM proteins (Charrin, et al., 2009; Sala-Valdes, et al., 2006) that bind $PI(4,5)P_2$ (Fehon, et al., 2010). Altogether these data indicate that the tetraspanin web is present in close proximity with $PI(4,5)P_2$ membrane domains and might regulate HIV-1 budding. To pursue this study, because of the small TNT diameter (<200 nm (Sowinski, et al., 2008)), it would be interesting to use a high resolution technique with a resolution <20-30 nm such as photo-activation localization microscopy for instance (Toomre and Bewersdorf, 2010).

Materials and Methods

Chemicals

DiD, DiI and fluorescent phalloidins were from Life Technologies. Human fibronectin and transferrin were from Sigma. Transferrin was labelled with Cy3 or Cy5 according to the instructions of the manufacturer (Life Technologies).

Plasmids

Mammalian expression vectors for the following constructs were obtained from the indicated individuals. YFP-αTubulin and YFP-KDEL were from Fabien Blanchet (CPBS, Montpellier), ezrin-GFP from Paul Mangeat, GFP-Cdc42 and GFP-Rac1 from Cécile Gauthier-Rouvière, GFP-Rab4 and GFP-Rab11 from Anne Blangy (CRBM, Montpellier), CD9-GFP and CD81-mCherry from Pierre-Emmanuel Milhiet (CBS, Montpellier), GFP-N-WASP from Pascale Cossart (Institut Pasteur, Paris), $PH_{PLC\delta}$ R40L-GFP from Tamas Balla (NIH, Bethesda), GFP-Exo70 from Wei Guo (University of Pennsylvania, Philadelphia), GFP-M-Sec

from Hiroshi Ohno (RIKEN, Kanagawa), MIM-I-Bar-GFP from Pekka Lappalainen (Institute of Biotechnology, Helsinki), GFP-Rab35 from Arnaud Echard (Institut Pasteur Paris). pEGFP was from Clontech and Gag-EGFP from the NIH AIDS reagent program. The GFP chimera of $PH_{PLC\delta}$ and PH_{Akt} were described before (Rayne, et al., 2010).

Cell transfection and TNT observation

Jurkat T-cells were used throughout this study. Cell labelling with DiD or DiI was performed as described (Sowinski, et al., 2011). Cells were transfected by electroporation (Vendeville, et al., 2004) before plating $0.8.10^6$ cells in 1 ml of medium onto 18 mm-diameter coverslips in 12-well plates. Coverslips were previously coated with fibronectin (10 µg/ml PBS). After overnight incubation, cells were either imaged directly or washed gently twice with PBS containing 0.1% paraformaldehyde before fixation in 3.7 % paraformaldehyde for 2 h at RT. Following treatment with 50 mM ammonium chloride, cells were either mounted directly or permeabilized with saponin for labelling F-actin with phalloidin (Rayne, et al., 2010). Samples were imaged using an SPE Leica confocal microscope with a 63x objective (NA 1.33). Confocal sections were centred on the TNT and were ~2 µm thick.

FRAP

Jurkat cells were transfected as described above and plated on fibronectin-coated 35 mm diameter glass-bottom Ibidi dishes. After overnight incubation, the medium was changed to medium without phenol red and 10 mM Hepes was added before imaging at 37°C using a Zeiss LSM780 confocal microscope and a 63x (NA 1.4) objective. Bleached area were circles of diameter between 0.4 and 4 μm^2, bleaching time was < 1.5 s, scanning times were < 100 ms and images were collected with an interval of ~0.2 s. 12 bits images were recorded. Calculations were performed using imageJ, using when needed a correction for scanning-induced bleaching that remained < 15% of initial fluorescence intensity. A simplified equation was used to obtain diffusion coefficients from confocal FRAP data (Kang, et al., 2012). Experimental D values were not corrected for membrane curvature (see Results).

Author contribution

CC prepared plasmids and performed some transfection experiments. SL was in charge of cell imaging. BB did some imaging, directed the study and wrote the paper.

Acknowledgements

We acknowledge all the people that provided expression vectors for this study, Daniel Davis and Patrick Bron for discussions, Virginie Georget and Sylvain de Rossi for help with FRAP and live cell imaging, respectively, Pierre-Emmanuel Milhiet for carefully reading the manuscript and Cyril Favard for help with FRAP analysis. This work was funded by Sidaction and the CNRS through the PEPS program.

References

Abounit, S. and Zurzolo, C. (2012) Wiring through tunneling nanotubes--from electrical signals to organelle transfer. J Cell Sci **125**, 1089-1098.

Amieva, M.R. and Furthmayr, H. (1995) Subcellular localization of moesin in dynamic filopodia, retraction fibers, and other structures involved in substrate exploration, attachment, and cell-cell contacts. Exp Cell Res **219**, 180-196.

Astoul, E., Edmunds, C., Cantrell, D.A. and Ward, S.G. (2001) PI 3-K and T-cell activation: limitations of T-leukemic cell lines as signaling models. Trends Immunol **22**, 490-496.

Bannai, H., Inoue, T., Nakayama, T., Hattori, M. and Mikoshiba, K. (2004) Kinesin dependent, rapid, bi-directional transport of ER sub-compartment in dendrites of hippocampal neurons. J Cell Sci **117**, 163-175.

Bell, N.M. and Lever, A.M. (2013) HIV Gag polyprotein: processing and early viral particle assembly. Trends Microbiol **21**, 136-144.

Berditchevski, F., Tolias, K.F., Wong, K., Carpenter, C.L. and Hemler, M.E. (1997) A novel link between integrins, transmembrane-4 superfamily proteins (CD63 and CD81), and phosphatidylinositol 4-kinase. J Biol Chem **272**, 2595-2598.

Charrin, S., le Naour, F., Silvie, O., Milhiet, P.E., Boucheix, C. and Rubinstein, E. (2009) Lateral organization of membrane proteins: tetraspanins spin their web. Biochem J **420**, 133-154.

Chinnery, H.R., Pearlman, E. and McMenamin, P.G. (2008) Cutting edge: Membrane nanotubes in vivo: a feature of MHC class II+ cells in the mouse cornea. J Immunol **180**, 5779-5783.

Davis, D.M. and Sowinski, S. (2008) Membrane nanotubes: dynamic long-distance connections between animal cells. Nat Rev Mol Cell Biol **9**, 431-436.

De Joussineau, C., Soule, J., Martin, M., Anguille, C., Montcourrier, P. and Alexandre, D. (2003) Delta-promoted filopodia mediate long-range lateral inhibition in Drosophila. Nature **426**, 555-559.

Di Paolo, G. and De Camilli, P. (2006) Phosphoinositides in cell regulation and membrane dynamics. Nature **443**, 651-657.

Espenel, C., Margeat, E., Dosset, P., Arduise, C., Le Grimellec, C., Royer, C.A., Boucheix, C., Rubinstein, E. and Milhiet, P.E. (2008) Single-molecule analysis of CD9 dynamics and partitioning reveals multiple modes of interaction in the tetraspanin web. J Cell Biol **182**, 765-776.

Faure, S., Salazar-Fontana, L.I., Semichon, M., Tybulewicz, V.L., Bismuth, G., Trautmann, A., Germain, R.N. and Delon, J. (2004) ERM proteins regulate cytoskeleton relaxation promoting T cell-APC conjugation. Nat Immunol **5**, 272-279.

Fehon, R.G., McClatchey, A.I. and Bretscher, A. (2010) Organizing the cell cortex: the role of ERM proteins. Nat Rev Mol Cell Biol **11**, 276-287.

Fuller, S.D., Wilk, T., Gowen, B.E., Krausslich, H.G. and Vogt, V.M. (1997) Cryo-electron microscopy reveals ordered domains in the immature HIV-1 particle. Curr Biol **7**, 729-738.

Golebiewska, U., Nyako, M., Woturski, W., Zaitseva, I. and McLaughlin, S. (2008) Diffusion coefficient of fluorescent phosphatidylinositol 4,5-bisphosphate in the plasma membrane of cells. Mol Biol Cell **19**, 1663-1669.

Golebiewska, U., Kay, J.G., Masters, T., Grinstein, S., Im, W., Pastor, R.W., Scarlata, S. and McLaughlin, S. (2011) Evidence for a fence that impedes the diffusion of phosphatidylinositol 4,5-bisphosphate out of the forming phagosomes of macrophages. Mol Biol Cell **22**, 3498-3507.

Hammond, G.R., Sim, Y., Lagnado, L. and Irvine, R.F. (2009) Reversible binding and rapid diffusion of proteins in complex with inositol lipids serves to coordinate free movement with spatial information. J Cell Biol **184**, 297-308.

Hase, K., Kimura, S., Takatsu, H., Ohmae, M., Kawano, S., Kitamura, H., Ito, M., Watarai, H., Hazelett, C.C., Yeaman, C. and Ohno, H. (2009) M-Sec promotes membrane nanotube formation by interacting with Ral and the exocyst complex. Nat Cell Biol **11**, 1427-1432.

Heasman, S.J. and Ridley, A.J. (2008) Mammalian Rho GTPases: new insights into their functions from in vivo studies. Nat Rev Mol Cell Biol **9**, 690-701.

Helma, J., Schmidthals, K., Lux, V., Nuske, S., Scholz, A.M., Krausslich, H.G., Rothbauer, U. and Leonhardt, H. (2012) Direct and dynamic detection of HIV-1 in living cells. PLoS One 7, e50026.

Hermida-Matsumoto, L. and Resh, M.D. (2000) Localization of human immunodeficiency virus type 1 Gag and Env at the plasma membrane by confocal imaging. J Virol **74**, 8670-8679.

Igakura, T., Stinchcombe, J.C., Goon, P.K., Taylor, G.P., Weber, J.N., Griffiths, G.M., Tanaka, Y., Osame, M. and Bangham, C.R. (2003) Spread of HTLV-I between lymphocytes by virus-induced polarization of the cytoskeleton. Science **299**, 1713-1716.

Jouvenet, N., Bieniasz, P.D. and Simon, S.M. (2008) Imaging the biogenesis of individual HIV-1 virions in live cells. Nature **454**, 236-240.

Kang, M., Day, C.A., Kenworthy, A.K. and DiBenedetto, E. (2012) Simplified equation to extract diffusion coefficients from confocal FRAP data. Traffic **13**, 1589-1600.

Krementsov, D.N., Weng, J., Lambele, M., Roy, N.H. and Thali, M. (2009) Tetraspanins regulate cell-to-cell transmission of HIV-1. Retrovirology **6**, 64.

Lamb, R.F., Ozanne, B.W., Roy, C., McGarry, L., Stipp, C., Mangeat, P. and Jay, D.G. (1997) Essential functions of ezrin in maintenance of cell shape and lamellipodial extension in normal and transformed fibroblasts. Curr Biol **7**, 682-688.

Lehmann, M.J., Sherer, N.M., Marks, C.B., Pypaert, M. and Mothes, W. (2005) Actin- and myosin-driven movement of viruses along filopodia precedes their entry into cells. J Cell Biol **170**, 317-325.

Liu, J., Zuo, X., Yue, P. and Guo, W. (2007) Phosphatidylinositol 4,5-bisphosphate mediates the targeting of the exocyst to the plasma membrane for exocytosis in mammalian cells. Mol Biol Cell **18**, 4483-4492.

Liu, J., Zhao, Y., Sun, Y., He, B., Yang, C., Svitkina, T., Goldman, Y.E. and Guo, W. (2012) Exo70 stimulates the Arp2/3 complex for lamellipodia formation and directional cell migration. Curr Biol 22**,** 1510-1515.

Martin-Serrano, J. and Neil, S.J. (2011) Host factors involved in retroviral budding and release. Nat Rev Microbiol **9**, 519-531.

Mitra, S., Cheng, K.W. and Mills, G.B. (2011) Rab GTPases implicated in inherited and acquired disorders. Semin Cell Dev Biol **22**, 57-68.

Murooka, T.T., Deruaz, M., Marangoni, F., Vrbanac, V.D., Seung, E., von Andrian, U.H., Tager, A.M., Luster, A.D. and Mempel, T.R. (2012) HIV-infected T cells are migratory vehicles for viral dissemination. Nature **490**, 283-287.

Nobile, C., Rudnicka, D., Hasan, M., Aulner, N., Porrot, F., Machu, C., Renaud, O., Prevost, M.C., Hivroz, C., Schwartz, O. and Sol-Foulon, N. (2010) HIV-1 Nef inhibits ruffles, induces filopodia, and modulates migration of infected lymphocytes. J Virol **84**, 2282-2293.

Ohno, H., Hase, K. and Kimura, S. (2010) M-Sec: Emerging secrets of tunneling nanotube formation. Commun Integr Biol **3**, 231-233.

Onfelt, B., Nedvetzki, S., Yanagi, K. and Davis, D.M. (2004) Cutting edge: Membrane nanotubes connect immune cells. J Immunol **173**, 1511-1513.

Onfelt, B., Nedvetzki, S., Benninger, R.K., Purbhoo, M.A., Sowinski, S., Hume, A.N., Seabra, M.C., Neil, M.A., French, P.M. and Davis, D.M. (2006) Structurally distinct membrane nanotubes between human macrophages support long-distance vesicular traffic or surfing of bacteria. J Immunol **177**, 8476-8483.

Ono, A. (2010) Relationships between plasma membrane microdomains and HIV-1 assembly. Biol Cell 102, 335-350.

Ott, D.E., Coren, L.V., Kane, B.P., Busch, L.K., Johnson, D.G., Sowder, R.C., 2nd, Chertova, E.N., Arthur, L.O. and Henderson, L.E. (1996) Cytoskeletal proteins inside human immunodeficiency virus type 1 virions. J Virol **70**, 7734-7743.

Rayne, F., Debaisieux, S., Yezid, H., Lin, Y.L., Mettling, C., Konate, K., Chazal, N., Arold, S.T., Pugniere, M., Sanchez, F., Bonhoure, A., Briant, L., Loret, E., Roy, C. and Beaumelle, B. (2010) Phosphatidylinositol-(4,5)-bisphosphate enables efficient secretion of HIV-1 Tat by infected T-cells. EMBO J **29**, 1348-1362.

Rustom, A., Saffrich, R., Markovic, I., Walther, P. and Gerdes, H.H. (2004) Nanotubular highways for intercellular organelle transport. Science **303**, 1007-1010.

Sala-Valdes, M., Ursa, A., Charrin, S., Rubinstein, E., Hemler, M.E., Sanchez-Madrid, F. and Yanez-Mo, M. (2006) EWI-2 and EWI-F link the tetraspanin web to the actin cytoskeleton through their direct association with ezrin-radixin-moesin proteins. J Biol Chem **281**, 19665-19675.

Sherer, N.M., Lehmann, M.J., Jimenez-Soto, L.F., Horensavitz, C., Pypaert, M. and Mothes, W. (2007) Retroviruses can establish filopodial bridges for efficient cell-to-cell transmission. Nat Cell Biol **9**, 310-315.

Sowinski, S., Jolly, C., Berninghausen, O., Purbhoo, M.A., Chauveau, A., Kohler, K., Oddos, S., Eissmann, P., Brodsky, F.M., Hopkins, C., Onfelt, B., Sattentau, Q. and Davis, D.M. (2008) Membrane nanotubes physically connect T cells over long distances presenting a novel route for HIV-1 transmission. Nat Cell Biol **10**, 211-219.

Sowinski, S., Alakoskela, J.M., Jolly, C. and Davis, D.M. (2011) Optimized methods for imaging membrane nanotubes between T cells and trafficking of HIV-1. Methods **53**, 27-33.

Takenawa, T. and Suetsugu, S. (2007) The WASP-WAVE protein network: connecting the membrane to the cytoskeleton. Nat Rev Mol Cell Biol **8**, 37-48.

Thrasher, A.J. and Burns, S.O. (2010) WASP: a key immunological multitasker. Nat Rev Immunol **10**, 182-192.

Toomre, D. and Bewersdorf, J. (2010) A new wave of cellular imaging. Annu Rev Cell Dev Biol **26**, 285-314.

van den Bogaart, G., Meyenberg, K., Risselada, H.J., Amin, H., Willig, K.I., Hubrich, B.E., Dier, M., Hell, S.W., Grubmuller, H., Diederichsen, U. and Jahn, R. (2011) Membrane protein sequestering by ionic protein-lipid interactions. Nature **479**, 552-555.

Van Engelenburg, S.B., Shtengel, G., Sengupta, P., Waki, K., Jarnik, M., Ablan, S.D., Freed, E.O., Hess, H.F. and Lippincott-Schwartz, J. (2014) Distribution of ESCRT machinery at HIV assembly sites reveals virus scaffolding of ESCRT subunits. Science **343**, 653-656.

Varnai, P. and Balla, T. (1998) Visualization of phosphoinositides that bind pleckstrin homology domains: calcium- and agonist-induced dynamic changes and relationship to myo-[3H]inositol-labeled phosphoinositide pools. J Cell Biol **143**, 501-510.

Vendeville, A., Rayne, F., Bonhoure, A., Bettache, N., Montcourrier, P. and Beaumelle, B. (2004) HIV-1 Tat enters T cells using coated pits before translocating from acidified endosomes and eliciting biological responses. Mol Biol Cell **15**, 2347-2360.

Zhao, H., Pykalainen, A. and Lappalainen, P. (2011) I-BAR domain proteins: linking actin and plasma membrane dynamics. Curr Opin Cell Biol **23**, 14-21.

Zhao, Y., Liu, J., Yang, C., Capraro, B.R., Baumgart, T., Bradley, R.P., Ramakrishnan, N., Xu, X., Radhakrishnan, R., Svitkina, T. and Guo, W. (2013) Exo70 generates membrane curvature for morphogenesis and cell migration. Dev Cell **26**, 266-278.

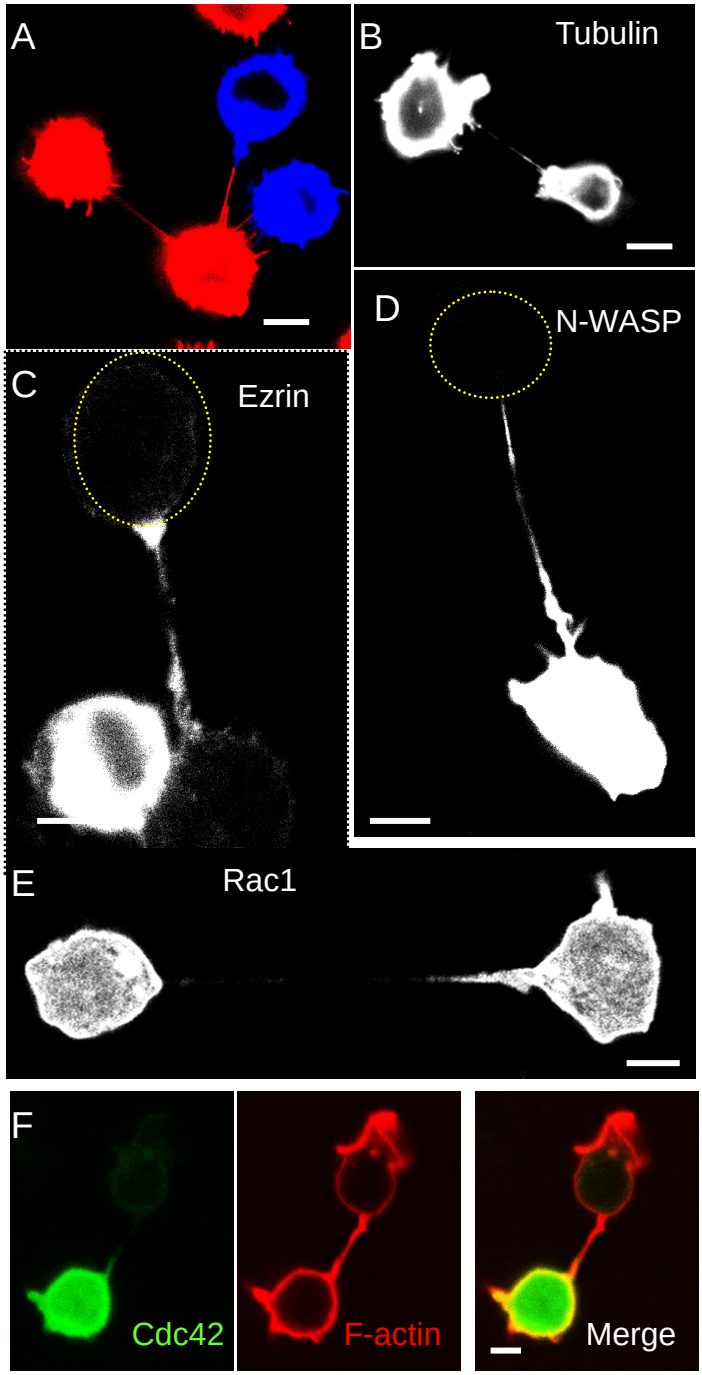

Figure 1. Actin, ezrin and N-WASP are enriched in T-cell TNTs. (A) Jurkat T-cells were labelled with a lipophilic dye DiD (blue) or DiI (red). The two populations were then mixed (1/1), layered on fibronectin coated coverslips, fixed after overnight incubation and imaged by confocal microscopy. (B-F) Jurkat cells were transfected with (B) YFP-Tubulin and CD81-mcherry, (C) ezrin-GFP, (D) GFP-N-WASP, (E) GFP-Rac1 or (F) GFP-Cdc42 before overnight incubation, fixation and imaging. When indicated cells were permeabilized for F-actin staining with fluorescent phalloidin. Connected cell bodies are indicated by ellipses in some images that are representative of 20 (A), 6 (B), 11 (C), 13 (D), 13 (E) and 7 (F) nanotubes. Bars, 5 µm.

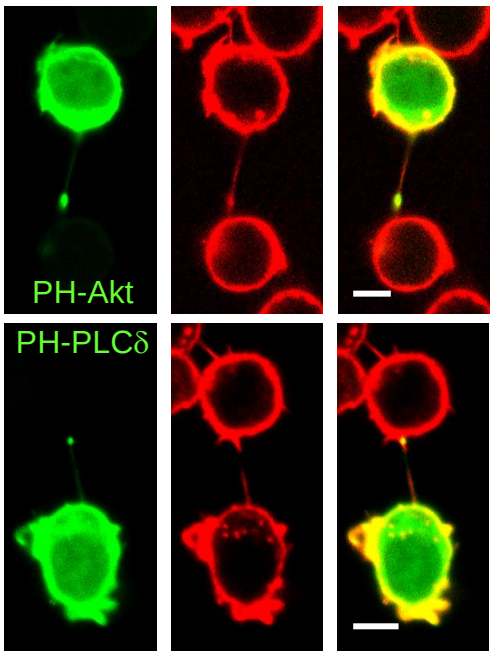

Figure 2. PI(4,5)P_2 and PI(4,5)P_3 are enriched at the tip of TNTs. Jurkat cells were transfected as indicated with the GFP chimera of PH-PLCδ that binds PI(4,5)P_2, or PH-Akt that recognizes PI(3,4,5)P_3. F-actin was stained with fluorescent phalloidin. Quantification showed that 29 / 42 TNTs (PH-PLCδ) and 13 / 20 TNTs (PH-Akt) displayed a tracer accumulation at the TNT tip. Bars, 5 µm.

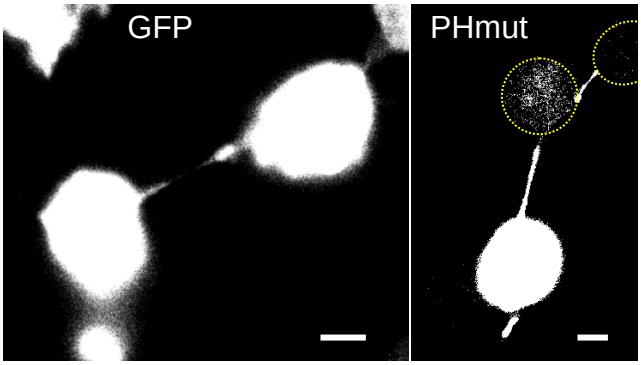

Figure 3. Cytosolic proteins are present in T-cells TNTs. Jurkat cells were transfected with GFP or a GFP version of the R40L mutant of $PH_{PLC\delta}$ (PHmut) that is cytosolic (Varnai and Balla, 1998), as indicated. Connected cell bodies are indicated by ellipses when needed for visualization. Images are representative of 6 (GFP) or 8 (PHmut) TNTs. Bars, 5 µm.

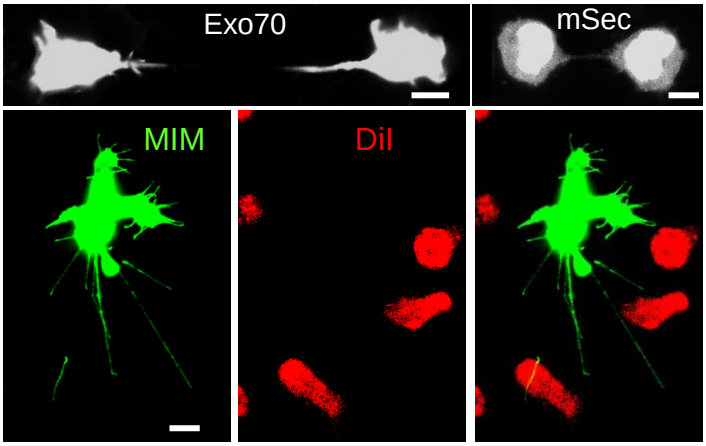

Figure 4. TNTs contain Exo70. Jurkat cells were transfected with the GFP chimera of Exo70, mSec or MIM-I-Bar. When indicated, transfected cells were mixed with DiI labelled cells. Images are representative of 15 (Exo70), 6 (mSec) or 15 (MIM) TNTs. Bars, 5 µm.

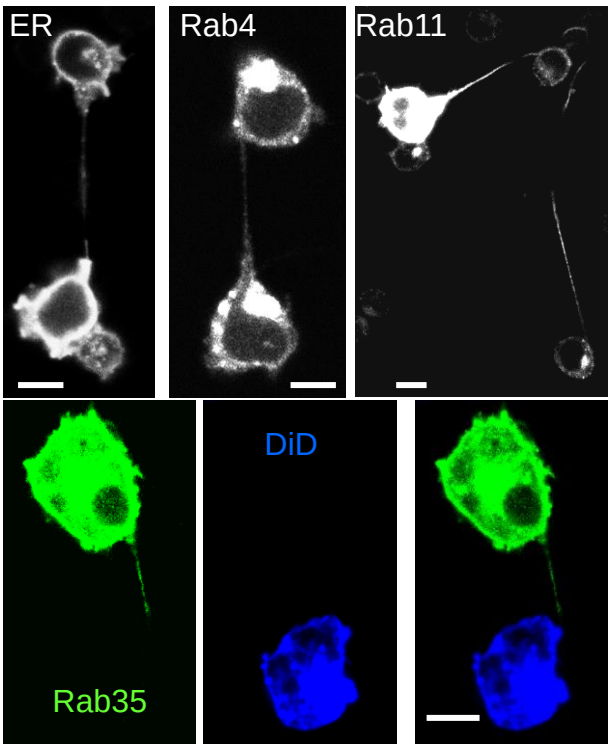

Figure 5. Endoplasmic reticulum and endocytic structures are not present within T-cells TNTs. Cells were transfected with YFP-KDEL or GFP-Rab proteins. When indicated, transfected cells were mixed (1/1) with DiD-labelled cells before adding onto fibronectin-coated coverslips. Images are representative of 6 (YFP-KDEL), 6 (Rab4) , 7 (Rab11) or 14 (Rab35) TNTs. Bars, 5 µm.

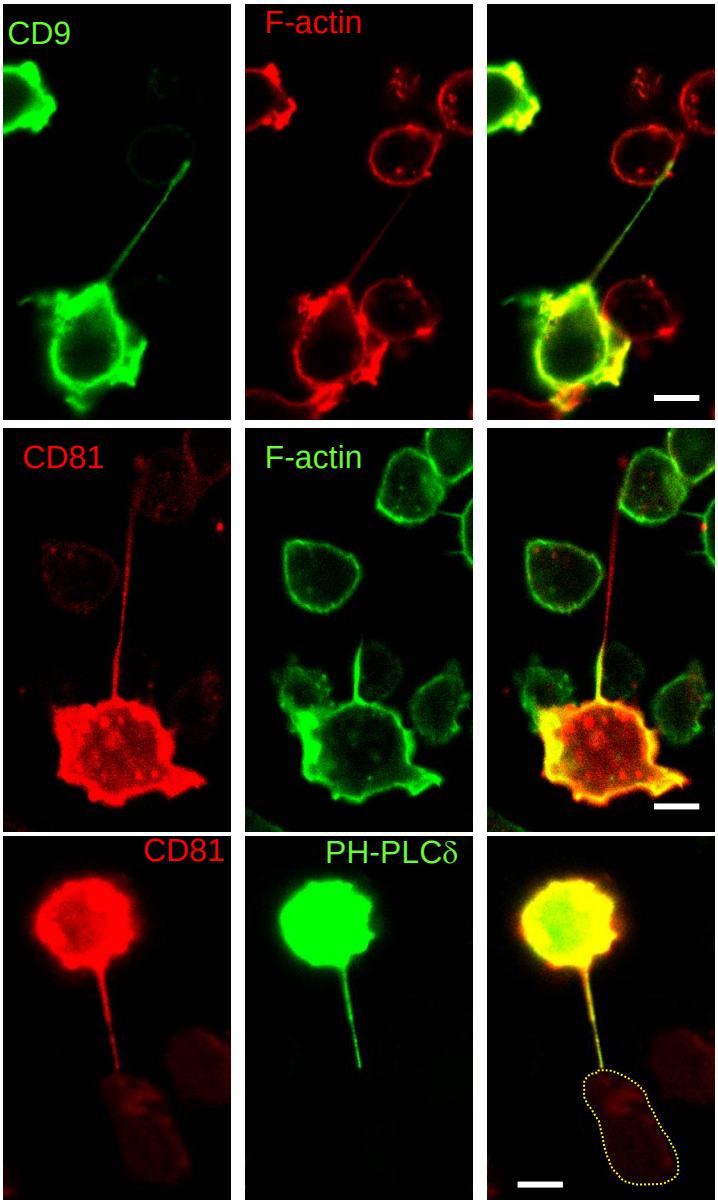

Figure 6. Tetraspanins are enriched in T-cell TNTs. Cells were transfected with CD9-GFP or CD81-mCherry with or without $PH_{PLC\delta}$-GFP as indicated, before overnight incubation on fibronectin-coated coverslips. When indicated, F-actin was stained with fluorescent phalloidin. The connected cell periphery is indicated by a dotted line when needed. Images are representative of 15 (CD9/actin), 17(CD81/actin) or 16 (CD81/ $PH_{PLC\delta}$) TNTs. Bars, 5 µm.

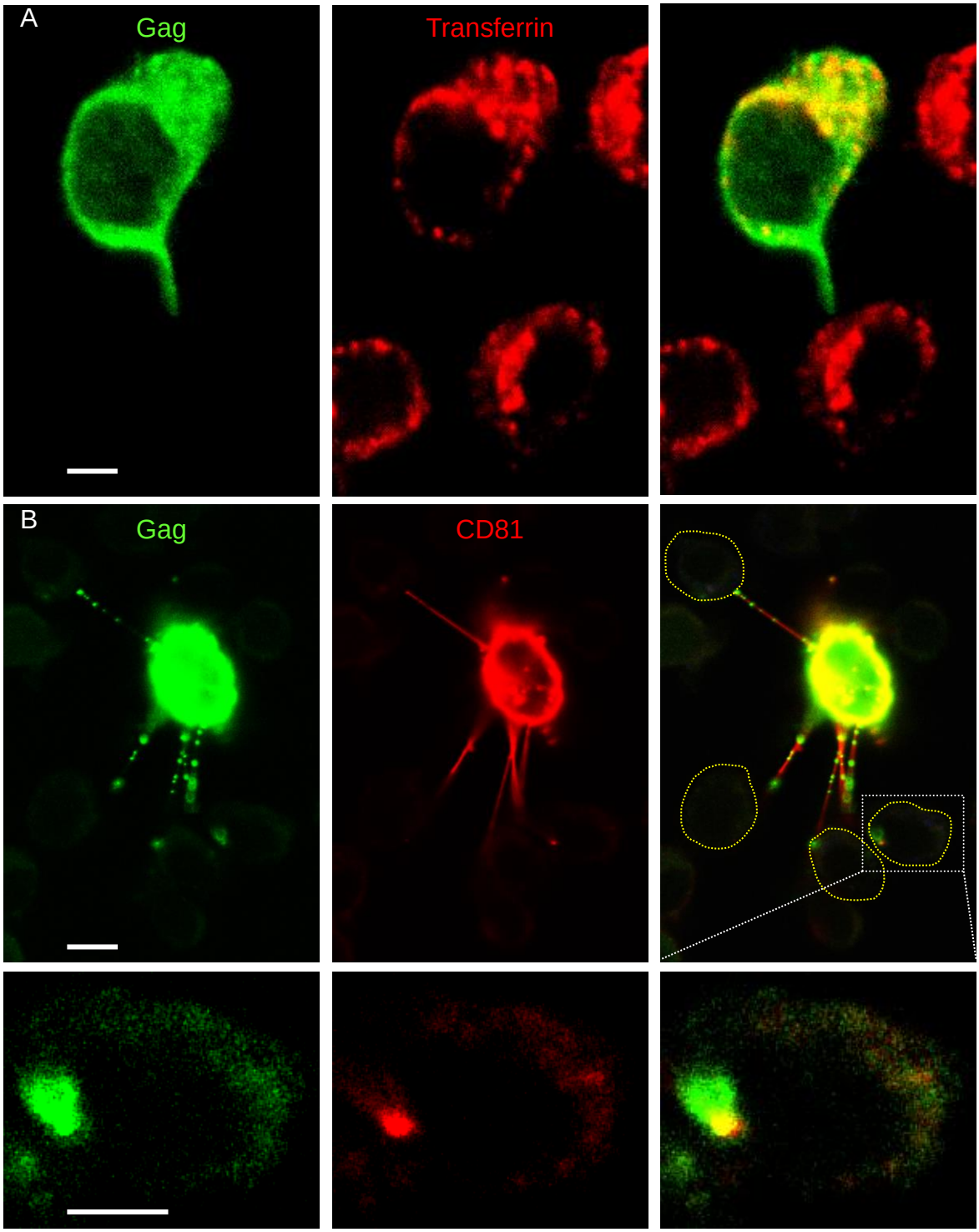

Figure 7. HIV-1 virus like particles assemble at the TNT tip. Jurkat cells were transfected with Gag-GFP without (A) or with (B) CD81-mcherry and incubated overnight onto fibronectin-coated coverslips. When indicated (A), 100 nM fluorescent transferrin was added 40 min before fixation. Transferrin is absent from TNTs. When needed (B) the connected cell periphery is indicated by a dotted line. 3 out of 4 TNTs with tips within the confocal section show a Gag-GFP spot on the connected cell. The boxed region is enlarged in the lowest panels. Images are representative of 7 (A) or 20 (B) TNTs. Bars, 5 µm.

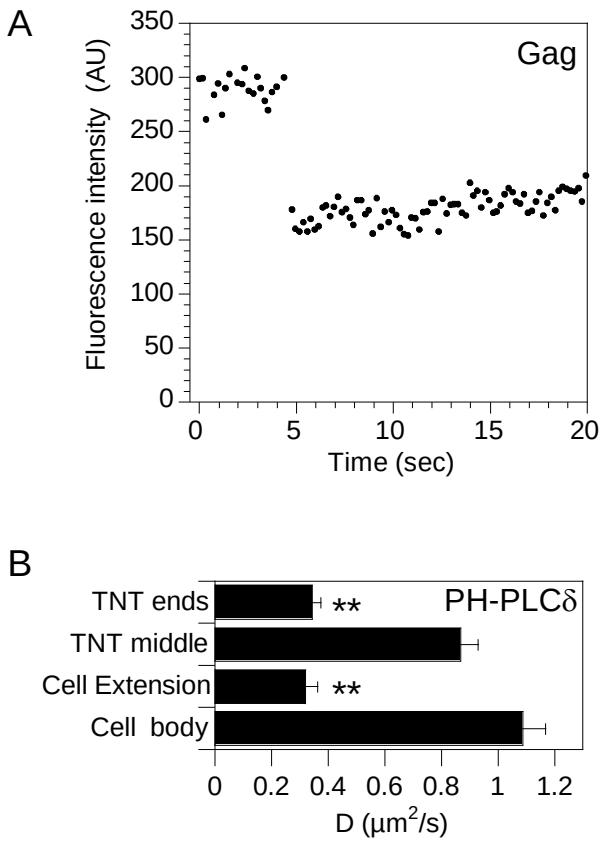

Figure 8. PI(4,5)P_2 mobility is reduced at the TNT tips. (A) Time trace of average fluorescence intensity per pixel in the bleached area of a representative TNT of a Gag-GFP transfected cell. (B) Fitted apparent diffusion coefficients (D) of $PH_{PLC\delta}$-GFP at the surface of cells, cell extensions, TNT middle or TNT ends, as indicated. Data are mean $\pm$ SE of ten independent measurements and the significance of differences was assessed using an unpaired, two-sided Student's t-test (**, $p < 0.01$).

Lachambre *et al.* Supplementary Figure 1.

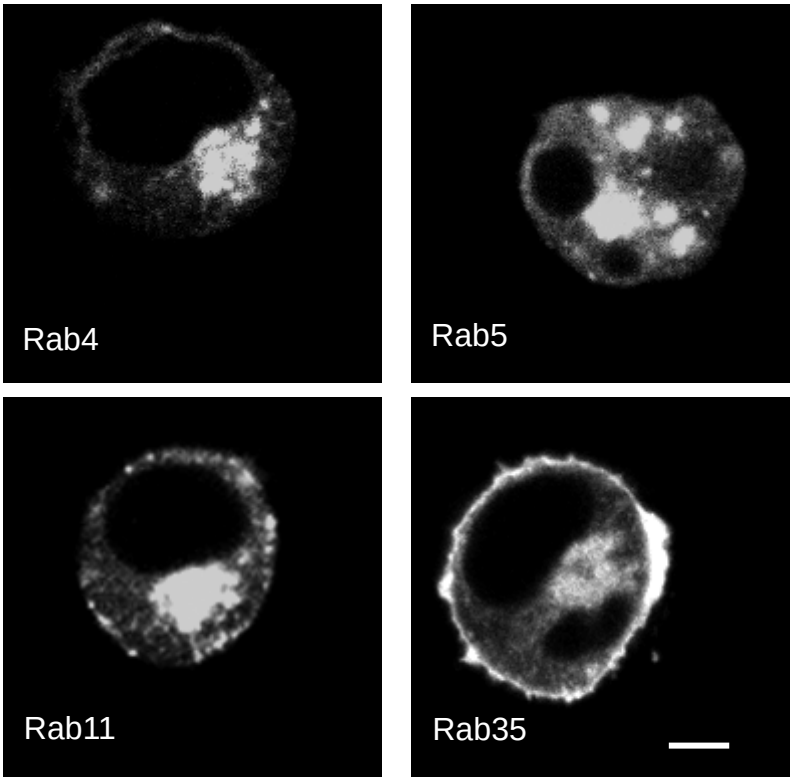

Localization of endocytic Rab proteins in Jurkat cells. Cells were transfected with the indicated GFP chimera before fixation and observation by confocal microscopy. Representative median optical section. Bar, 5 µm.